Additive manufacturing for novel structural health monitoring systems

Maria STRANTZA [1,2], Michael HINDERDAEL [2], Dieter DE BAERE [2],
Isabelle VANDENDAEL [3], Herman TERRYN [3],
Danny VAN HEMELRIJCK [1], Patrick GUILLAUME [2]

[1] Dpt Mechanics of Materials and Constructions, VUB (Vrije Universiteit Brussel), Pleinlaan 2, Brussels 1050 BELGIUM
Maria.Strantza@vub.ac.be, Danny.Van.Hemelrijck@vub.ac.be

[2] Dpt Mechanical Engineering, VUB (Vrije Universiteit Brussel), Pleinlaan 2, Brussels 1050 BELGIUM
Michael.Hinderdael@vub.ac.be, Dieter.De.Baere@vub.ac.be, Patrick.Guillaume@vub.ac.be

[3] Dpt Materials and Chemistry, VUB (Vrije Universiteit Brussel), Pleinlaan 2, Brussels 1050 BELGIUM
Isabelle.Vandendael@vub.ac.be, Herman.Terryn@vub.ac.be

Keywords: Smart structures, Additive manufacturing, Structural health monitoring, Industrial applications.

Abstract

Aerospace and automotive industries are some of the industrial sectors that are attracted to structural health monitoring (SHM) systems. An SHM system should be: (1) integrated from the beginning of the structural design, (2) reliable, (3) light-weight and (4) able to inspect critical parts that are not easily accessible. Additive manufacturing (AM) is receiving momentum during the last years from many industrial sectors. The increase in design freedom offered by AM can be used in order to develop lightweight and complex structures. Typically these structures cannot be easily produced by subtractive conventional methods. We developed a novel approach for SHM systems. Our approach is based on fusing the aforementioned technologies – SHM and AM. Our novel approach is called the effective Structural Health Monitoring (eSHM) system. The eSHM system detects cracks in a structure by means of an integrated network of pressurised capillaries. The latter is integrated into a metallic structure which is produced by AM. For benchmarking, in traditional specimens (not produced by AM), the capillary can be machined. The current system has proven its effectiveness. The main objective of this work is to investigate the fatigue response of structures with an integrated eSHM system and the effectiveness of the eSHM system. The reliability of the eSHM system is evaluated during four-point bending fatigue tests. In the framework of this investigation specimens with integrated capillaries produced by AM and conventional material are tested *with respect to the eSHM system. Furthermore, an optimization of various capillaries'* locations is also taking place. Heat treated conditions and autofrettaged conditions of samples are compared with conventional samples. It is concluded that an integrated eSHM system can be included on the initial design of an AM structure with promising results. The current system does not jeopardize the structural integrity of a structure while it enables one of the main challenges for SHM systems – SHM integration into the structure from the initial design.

1 INTRODUCTION

Fatigue is considered as one of the principle causes of failure in engineering structures. Besides the traditional inspections via non-destructive techniques, engineering sectors encourage to find novel solutions for continuous monitoring. Reliability and life-safety are two of the main parameters that must be enhanced. Structural health monitoring (SHM) is a damage detection method that can provide information about the structural integrity of an engineering structure under real operation conditions [1]. The objective of a SHM system is clearly the improvement of life-safety and the reduction of the operational cost which is a factor that is related to the maintenance cost [2]. During the past years, many investigations were conducted on developments of smart SHM systems which result in a vast amount of literature. The research on SHM systems has been particularly influenced by the biological nervous system [3], [4]. Smart structures demand integrated systems in order to enhance the functionality without compromising the continued monitoring of a structure. However, most of the SHM systems are in a development stage and many practical issues still remain.

Additive manufacturing (AM) is a relatively new and innovative manufacturing technology [5]. AM technology – commonly called three dimensional (3D) printing, has the potential to go beyond the design constraints of the conventional manufacturing technologies. In the future the limitations of AM will be further reduced and allow the design engineer to fully exploit his creativity. During the last decade, AM of metals is gaining momentum but it has taken years of research in order to get to the markets. Initially, machine developments and establishments of the processes, in order to get fully dense parts, were the major initial issues responsible for the delay. Nowadays, AM is introduced in industrial sectors such as automotive industry, aerospace, and medical industry. Laser metal deposition (LMD) is one of the main AM processes that is widely used for the production of metallic parts [9]. Despite the advantages of the light-weight and complex structures that are provided by AM, improvements in order to meet the high expectations of the markets are still needed. Production speed, cost, residual stresses and the quality of the structural integrity of the AM parts are the main drawbacks [6].

Undoubtedly, AM can produce smart engineering structures that cannot be produced by conventional subtractive production methods. In that aspect, Vrije Universiteit Brussels has developed a novel SHM system that is called effective structural health monitoring (eSHM) system [7], [8]. The current system uses the major advantages of the AM technologies and combines them with the beneficial usage of an SHM system. The functionality of the system is based on checking the absolute fluid pressure changes in a network of capillaries or cavities that are integrated into the interior of a metallic part. A pressure change in the network indicates the presence of a crack.

In this study, we are using four-point bending specimens with an integrated straight capillary. The capillary is located as close to the surface as possible. The primary aim of this investigation is to prove that the eSHM can successfully detect cracks in the current specimen specifications. The latter is related to the enhancement of the technological readiness level (TRL) 4. The TRL 4 is linked with the maturity of the system and was enabled in other studies [10]–[12]. Secondary objective is to investigate LMD samples in as-built and annealed conditions. Another parameter which might enhance the capillary robustness is the residual stress distribution around the capillary. To do so, autofrettage process is also applied on the capillary of a sample. As a final point, the results of the AM samples were compared with the fatigue response of conventional specimens with drilled capillaries.

2 EXPERIMENTAL SETUP AND MATERIALS

Four-point bending Ti6Al4V specimens with an integrated eSHM system were tested. Each specimen – AM and conventional – had an integrated straight capillary located in the tension part of the four-point bending specimen. The capillary diameter was 1.8 mm for the LMD samples and 2 mm for the conventional. The AM specimens were produced by LMD and machined to the final dimensions as can be seen in figure 1. The building direction (BD) of the samples is also indicated in figure 1. The location of the capillary was selected to be equal to a distance a from the surface of the specimen, same distance from the side and the bottom of the specimen. The geometry of the specimen and the a distances are illustrated in figure 1. In the current investigation, the distance a was chosen to be 2 and 3 mm. These locations were also theoretically evaluated by finite element simulations in another study [12]. For the conventional specimens, similar geometries of mill annealed Ti6Al4V specimens were machined and capillaries of 2 mm diameter were drilled by the conventional subtractive method of deep gun drilling. For the annealed conditions of the AM samples, a heat treatment of 2 hours for 530 °C was applied on two AM specimens with a = 2 mm. This heat treatment obtains stress relieved conditions without altering the microstructure. For the case of the autofrettaged specimen, a capillary of a = 3 mm was subjected to 10,000 bar pressure. The latter should result in a beneficial compressive stress state around the capillary which should have a positive influence on the capillary with respect to the crack nucleation. The autofrettage process can introduce compressive residual stresses in capillaries or tubes by subjecting them to an enormous pressure [13]. Consequently, autofrettage could significantly increase the magnitude of the beneficial stresses and further fortify the capillary region.

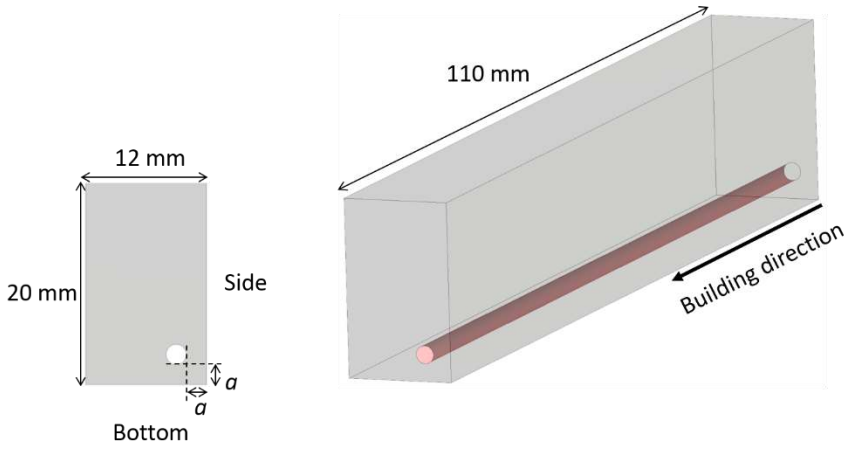

Figure 1: Cross-section of the capillary (a = 1.8 mm) positioned at distance a from the specimen's surface.

After machining (figure 2(a)), the specimens were equipped with a pressure transducer at one side and with a check valve at the other side. Before the installation of the check valve, a thread sealant was applied between the specimen and the check valve. After sealing, by means of the adhesive, the capillary was partially evacuated by means of a vacuum pump, keeping it at an under-pressure of 0.5 bar. For the final step, a stop was installed in the check valve as an additional occlusion. No leakages were present prior testing.

The specimens were subjected to a four-point bending cyclic fatigue loading with a frequency of 15 Hz and stress ratio (R) of 0.1. A schematic representation of the four-point bending fatigue test is depicted in figure 2(b). This test setup provides a uniform moment where shear forces are not present between the two inner loading points. The locations with the

likelihood of crack initiation were situated at the specimen's locations that were furthest away from the neutral axis – in the tension area of the four-point bending test. For the fatigue testing, the step-method was used [14]. According to the step method, the initial stress amplitude was chosen below the fatigue limit of the specimen. For each step a large number of cycles N (500,000 cycles) with the same stress level were applied. If failure does not occur the stress was increased with a specific step of approximately 80 MPa and again N numbers of cycles were applied. After the crack detection, each specimen was subjected to fatigue until the final failure. As a last step, fractographic analysis was performed on the fracture surface of each sample in order to verify the crack nucleation positions and identify the cause of failure.

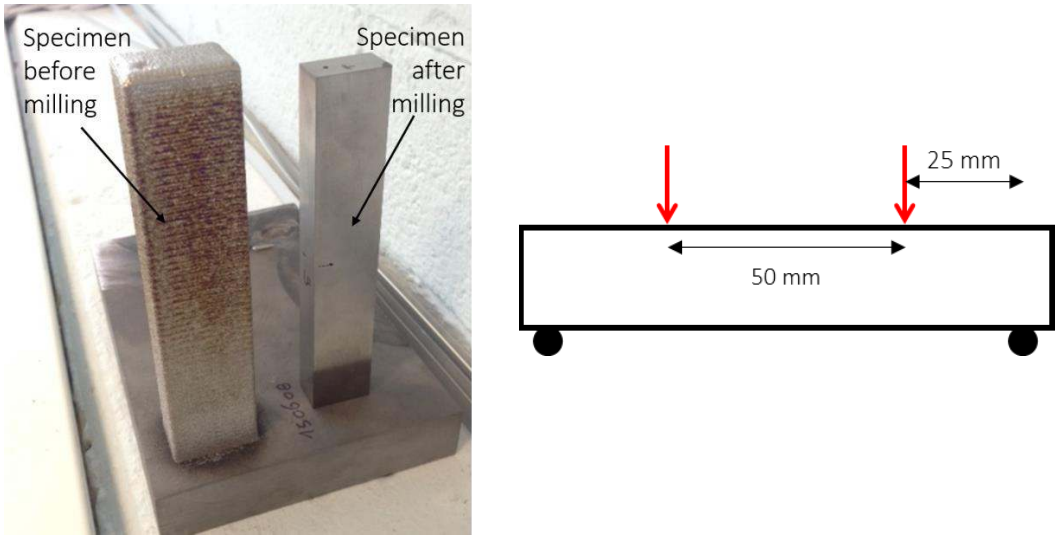

Figure 2: (a) Specimen after the LMD production and final specimen after machining. (b) Schematic representation of four-point bending setup.

3 RESULTS AND DISCUSSION

3.1 Pressure behaviour

The capillary pressure level was monitored by the pressure transducer of the eSHM system during the fatigue tests. When a crack penetrates the capillary, the pressure of the capillary is gradually increased. Consequently, the pre-set limit of the pressure sensor is reached and the fatigue test stops. Pre-set limit is the value that activates the stopping procedure of the controller of the test machine.

During the test, the pre-set limit was set at 0.7 bar. Figure 3 shows the pressure behaviour as a function of the time for the last second of the fatigue test for an annealed LMD specimen. A periodic discrepancy is depicted in the graph. This periodic character is linked to the crack opening and closing during fatigue. The pressure of the capillary increases and tends to reach the atmospheric pressure. Since the loading is cyclic and the crack opens for a fraction of each cycle, the pressure approaches atmospheric pressure in a stepwise manner. It should be noted that during the fatigue experiment and for 'sound' conditions – before a crack penetrates the capillary – the pressure is stable. This can be revealed from figure 4, where the pressure is stable at approximately 0.5 bar for a total fatigue life of 233,000 cycles.

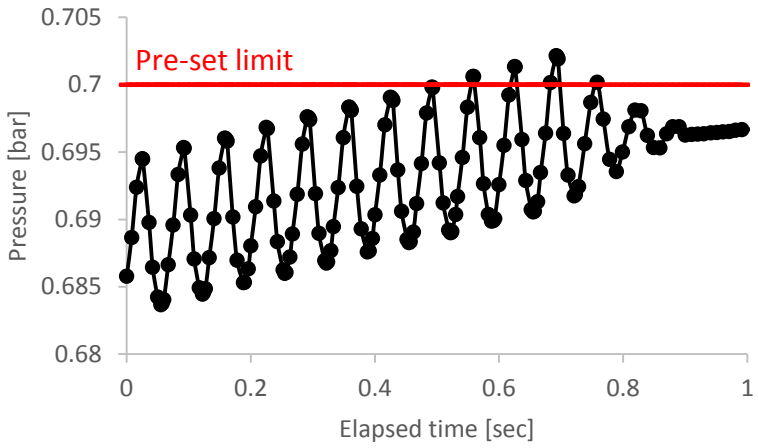

Figure 3: Pressure vs. elapsed time for an annealed LMD specimen during the last second of the fatigue test.

Figure 4: Pressure vs. total cycles during the fatigue life of an annealed LMD specimen.

3.2 Fatigue response

Seven LMD specimens and two conventional specimens with the integrated eSHM system at two different capillary locations were subjected to four-point bending fatigue tests. By using the step method, the fatigue life of the samples through the different stress steps was observed. Four specimens were tested in as-built conditions, two in annealed conditions and one autofrettaged specimen. An overview of the applied stresses and the number of cycles for the LMD specimens with the different capillary locations are shown in table 1, table 2 and table 3.

Two as-built specimens were tested for the 2 mm capillary location (table 1) and two as-built for the location of 3 mm (table 3). By comparing the values of the stress levels of the crack detection it is shown that the stress level increases significantly by increasing the capillary distance from the specimen's surface. The sample with 3 mm capillary location reached crack detection stress values that are 215 MPa higher in average. This is an expected result since the stress at the bottom of the capillary decreases when the capillary is located deeper in the specimen. The latter was also confirmed by simulation analysis presented in our previous investigation in [12]. For the case of the stress-relieved specimens, the capillary was

located on the closest distance to the edge, at a = 2 mm. From table 2 it is revealed that the fatigue life and the stress levels of crack detection did not indicate differences with the ones of the as-built components (table 1). Additional to the aforementioned tests, four-point bending tests were also applied on the autofrettaged LMD specimen with a capillary location of a = 3 mm. The specimen was investigated in order to study the influence of the beneficial residual stresses around the capillary region on the fatigue response and the crack nucleation locations. The autofrettaged specimen failed at the stress level of 740 MPa after 334,922 cycles. The current stress level and the fatigue life is in agreement with the stress level of crack detection of the as-built sample of the 3 mm capillary location. The latter might be an indication that the residual stress state did not affect the crack formation. However, further investigation with respect to the residual stress state around the capillary should be conducted.

Specimen 2 mm (AB)	Initial stress	Stress at crack detection	Cycles at crack detection
Sample 1	270 MPa	584 MPa	256,958
Sample 2	427 MPa	622 MPa	296,025

Table 1: Overview of the different steps and stress levels of the investigated as-built LMD Ti6Al4V specimens with an integrated straight capillary of 1.8 mm for the location of a = 2 mm.

Specimen 2 mm (SR)	Initial stress	Stress at crack detection	Cycles at crack detection
Sample 3	427 MPa	584 MPa	234,025
Sample 4	740 MPa	622 MPa	262,773

Table 2: Overview of the different steps and stress levels of the stress relieved LMD Ti6Al4V specimens with an integrated straight capillary of 1.8 mm for the location of a = 2 mm.

Specimen 3 mm (AB)	Initial stress	Stress at crack detection	Cycles at crack detection
Sample 1	427 MPa	897 MPa	248,296
Sample 2	740 MPa	740 MPa	257,021

Table 3: Overview of the different steps and stress levels of the stress relieved LMD Ti6Al4V specimens with an integrated straight capillary of 1.8 mm for the location of a = 3 mm.

Conventional specimens	Initial stress	Stress at crack detection	Cycles at crack detection
Sample 2 mm	584 MPa	976 MPa	384,270
Sample 3 mm	820 MPa	976 MPa	191,196

Table 4: Overview of the steps and the stress levels of conventional Ti6Al4V specimens with an integrated straight capillary of 1.8 mm for the location of of a = 2 mm and 3 mm.

Regarding the two conventional samples with the integrated straight capillaries, the cracks were detected in higher stress levels, compared to the LMD samples. Table 4 shows the obtained values for the conventional specimens with capillaries located at 2 mm and 3 mm locations. It is depicted from the results that the obtained stress levels were similar for both cases. In both specimens (3 and 2 mm capillary location), the crack was detected at the stress level of 976 MPa.

3.3 Fractographic analysis

The fracture surfaces of the cross-sections of all the specimens were examined by means of scanning electron microscope. Figure 5(a) shows the micrographs of a conventional sample where the capillary was located at 2 mm from the outer surface. The fractographic pictures of figure 5(a) reveal that in the case of the conventional specimen the crack nucleated at the edge of the specimens and not from the capillary. However, as it is depicted in figure 5(b) in the case of the autofrettaged LMD specimen the crack initiated at the capillary region. A close-up on the crack nucleation region shows that the crack nucleated from a sharp region between the layers. This region is probably caused by the layerwise manner of the AM process, and possibly high stress concentrations during fatigue eventually caused the crack nucleation. This behaviour was evident in all the LMD specimens. Furthermore, the observations depicted that no internal defects such as porosities were present around the capillary region.

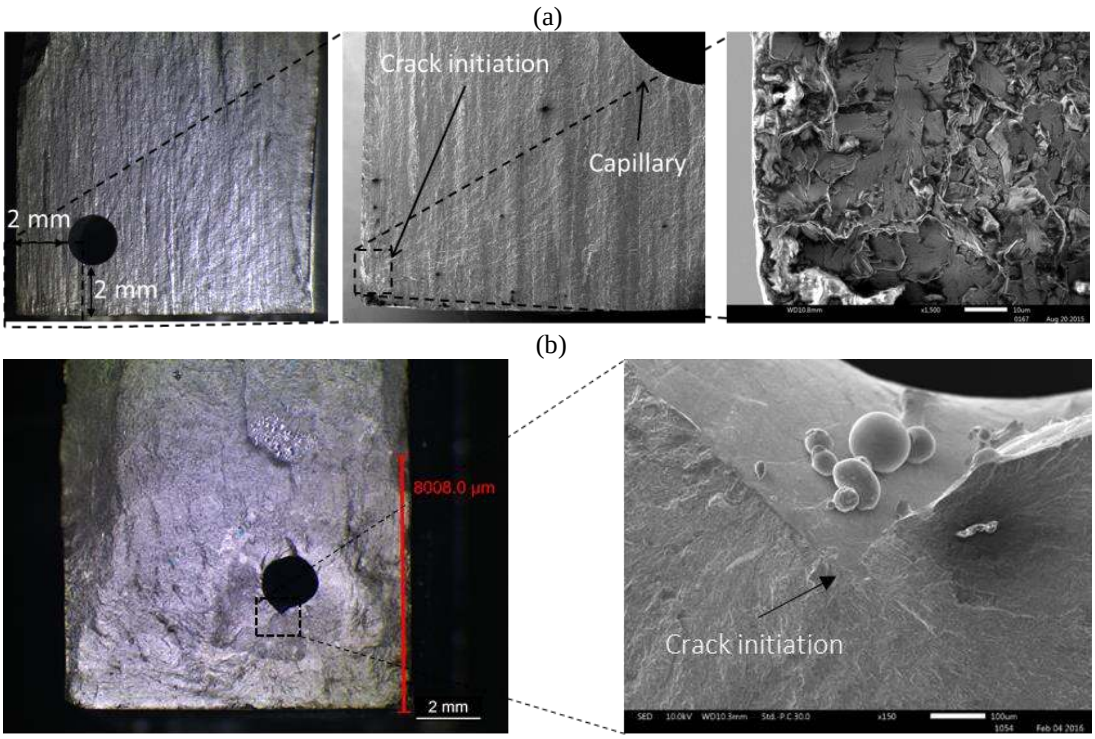

Figure 5: Scanning electron microscopy images of the cross-sections of the fracture surface of (a) a conventional Ti6Al4V specimen where the crack nucleated from the edge of the specimen and (b) an LMD autofrettaged sample with 3 mm capillary location with crack nucleation location at the capillary region.

The aforementioned observations highlight that the parameter of the capillary's roughness is more critical for crack nucleation than the residual stress state around the capillary region. Figure 6 shows the capillary region for the LMD and the conventional specimen. In the case of the LMD specimen (figure 6(a)) the roughness and the waviness of the capillary is significantly higher compared to the machined capillary of the conventional specimen (figure 6(b)). The surface finishing, R_a value, of the drilled capillary is in the range of 0.3 μm while for the LMD capillary is between 17.5 and 27 μm. Consequently, the roughness could affect the crack nucleation position. We can conclude that when the capillary is located close to the surface of the specimen (2 or 3 mm away), the roughness of the capillary is increasing the stress concentrations. As a result, the current configurations of the AM samples, are leading to crack nucleation from the capillary for stress levels above 584 MPa.

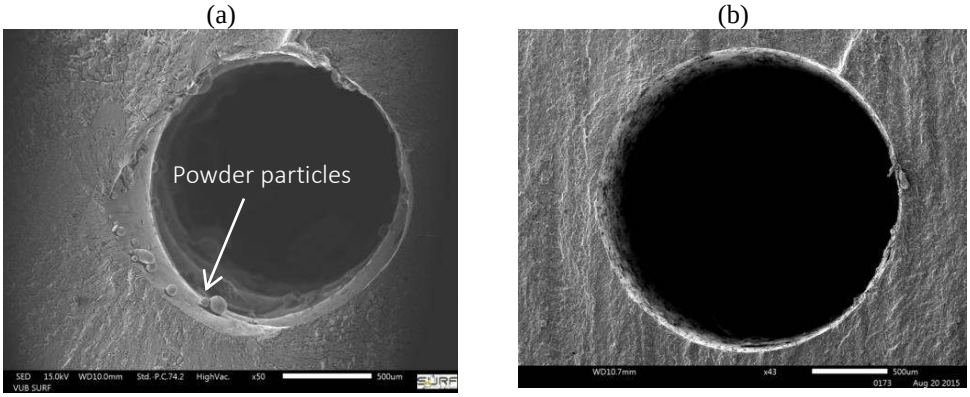

Figure 6: Capillary region of Ti6Al4V (a) produced by laser metal deposition with high roughness and (b) capillary produced by gun drilling on the conventional specimen with a fine surface finishing.

4 CONCLUSIONS

A novel structural health monitoring (SHM) system based on additive manufacturing (AM) was evaluated for straight elongated capillaries in laser metal deposited (LMD) Ti6Al4V. In this study, the effective SHM has again proven its effectiveness in crack detection under laboratory conditions. Both stress-relieved and as-built samples were tested. The capillaries were located as close as possible to the surface of the specimen. Locations of 2 mm and 3 mm – distances of the capillary from the outer surface of the sample – were evaluated. Furthermore, the AM fatigue results were compared with fatigue results from conventional Ti6Al4V specimens. The capillaries were located at the same positions and were drilled with a subtractive traditional method. A diameter of 1.8 mm for the LMD specimens and a diameter of 2 mm for the conventional specimens was selected. On the one hand, the experimental results demonstrated that for the locations of 2 mm and 3 mm in AM specimens, the capillary was crucial for crack initiation in high-stress levels (above 584 MPa). Stress relief did not improve the fatigue response. On the other hand, in the case of the ideal conditions of the conventional material – no internal defects, no residual stresses and fine surface finishing of the capillary – the crack nucleated from the side of the specimens and not from the capillary region. For the current specifications, it was concluded that the roughness of the capillary on the AM specimens increased the stress concentrations on the capillary regions. Future investigations on the surface roughness finishing of the capillary should be conducted in order to further elaborate on the crack nucleation behaviour. We will also focus on the improvements of the current technological readiness level of the eSHM system and on the integration of the novel eSHM system in a real mechanical application such as a gear or another mechanical part.

ACKNOWLEDGMENT

Research funded by an SBO Project grant 110070: eSHM with AM of the Agency for Innovation by Science and Technology (IWT).

REFERENCES

[1] C. R. Farrar and K. Worden, “An introduction to structural health monitoring.,” Philos. Trans. A. Math. Phys. Eng. Sci., vol. 365, no. 1851, pp. 303–15, Feb. 2007.

[2] H. Speckmann and H. Roesner, “Structural Health Monitoring : A Contribution to the Intelligent Aircraft Structure,” Proc. ECNDT 2006, pp. 1–7, 2006.

[3] N. Sharp, A. Kuntz, C. Brubaker, S. Amos, W. Gao, G. Gupta, A. Mohite, C. Farrar, and D. Mascareñas, “A bio-inspired asynchronous skin system for crack detection applications,” Smart Mater. Struct., vol. 23, no. 5, p. 055020, 2014.

[4] Salowitz, Guo, Roy, Nardari, Li, Kim, Kopsaftopoulos, and Chang, “A vision on stretchable bio-inspired networks for intelligent structures,” in International Workshop on Structural Health Monitoring, 2013.

[5] T. Wohlers and T. Gornet, “History of additive manufacturing,” Wohlers Rep. 2012, pp. 1–26, 2012.

[6] G. N. Levy, R. Schindel, and J. P. Kruth, “Rapid manufacturing and rapid tooling with Layer Manufacturing (LM) technologies, state of the art and future perspectives,” CIRP Ann. - Manuf. Technol., vol. 52, no. 2, pp. 589–609, Jan. 2003.

[7] D. De Baere, “Effective structural health monitoring” WO2014180870 A9, 31 December 2014.

[8] D. De Baere, M. Strantza, W. Devesse, and P. Guillaume, “Effective Structural Health Monitoring with Additive Manufacturing, In Proceedings of the EWSHM-7th European Workshop on Structural Health Monitoring, Nantes, France, 8–11 July.”

[9] D. D. Gu, W. Meiners, K. Wissenbach, and R. Poprawe, “Laser additive manufacturing of metallic components: materials, processes and mechanisms,” Int. Mater. Rev., vol. 57, no. 3, pp. 133–164, May 2012.

[10] M. Strantza, D. De Baere, M. Rombouts, G. Maes, D. Van Hemelrijck, and P. Guillaume, “Feasibility study on integrated structural health monitoring system produced by three-dimensional printing,” Struct. Heal. Monit. J., 2015.

[11] M. Strantza, D. De Baere, M. Rombouts, S. Clijsters, H. Terryn, P. Guillaume, D. Van Hemelrijck, M. Strantza, D. De Baere, M. Rombouts, S. Clijsters, I. Vandendael, M. Structures, and L. Cam, “3D Printing for Intelligent Metallic Structures,” 2015.

[12] M. Strantza, R. Vafadari, D. De Baere, M. Rombouts, I. Vandendael, H. Terryn, M. Hinderdael, A. Rezaei, W. Van Paepegem, P. Guillaume, and D. Van Hemelrijck, “Evaluation of Different Topologies of Integrated Capillaries in Effective Structural Health Monitoring System Produced by 3D Printing Evaluation of Different Topologies of Integrated Capillaries in Effective Structural Health Monitoring System Produced by,” in 10th International Workshop on Structural Health Monitoring.

[13] A. P. Parker, “Autofrettage of Open-End Tubes—Pressures, Stresses, Strains, and Code Comparisons,” J. Press. Vessel Technol., vol. 123, no. 3, p. 271, 2001.

[14] R. Bellows, S. Muju, and T. Nicholas, “Validation of the step test method for generating Haigh diagrams for Ti–6Al–4V,” Int. J. Fatigue, vol. 21, pp. 687–697, 1999.